Bulletin of Mathematical Biology (2022) 84:124
https://doi.org/10.1007/s11538-022-01083-7

Society for Mathematical Biology

ORIGINAL ARTICLE


# Time-Scale Analysis and Parameter Fitting for Vector-Borne Diseases with Spatial Dynamics

**Larissa Sartori**[1,2] · **Marcone Pereira**[1] · **Sergio Oliva**[1]

Received: 25 February 2021 / Accepted: 7 September 2022


**Abstract**
Vector-borne diseases are progressively spreading in a growing number of countries, and it has the potential to invade new areas and habitats. From the dynamical perspective, the spatial–temporal interaction of models that try to adjust to such events is rich and challenging. The first challenge is to address the dynamics of vectors (very fast and local) and the dynamics of humans (very heterogeneous and non-local). The objective of this work is to use the well-known Ross–Macdonald models, identifying different time scales, incorporating human spatial movements and estimate in a suitable way the parameters. We will concentrate on a practical example, a simplified space model, and apply it to dengue spread in the state of Rio de Janeiro, Brazil.

**Keywords** Vector-borne diseases · Time-scale analysis · Human mobility · Parameter fitting · Dengue

## 1 Introduction

Infectious diseases are currently a major cause of concern due to its high potential of dissemination (Peixoto et al. 2020). Vector-borne diseases may spread more slowly than those of direct transmission; however, due to lack of vaccination, basic sanitation, climate changes, and with increasing human mobility, such diseases are spreading and appearing in new regions, where the climate favors the proliferation of vectors (Gubler 2002; Liang et al. 2015; Bomfim et al. 2020). In addition, and considering that mosquitoes do not travel long distances, the human population is carrying the disease to places where mosquitoes are susceptible, which may lead to changes of

✉ Larissa Sartori
larissa.sartori@fgv.br

1 Department of Applied Mathematics, IME-USP, Institute of Mathematics and Statistics, University of São Paulo, Rua do Matão, 1010, São Paulo CEP 05508-090, Brazil

2 Department of Technology and Data Science, Fundação Getulio Vargas, São Paulo School of Business Administration, FGV-EAESP, Rua Itapeva, 474, Bela Vista, São Paulo CEP 01332-000, Brazil

Published online: 19 September 2022

the disease dynamics and increase the population heterogeneity (Iggidr et al. 2017). Mosquitoes of the species *Aedes aegypti* and *Aedes albopictus* are the most responsible for virus transmission, such as dengue, Zika, Chikungunya and Yellow Fever (Liu-Helmersson et al. 2016; Kraemer et al. 2015). For instance, we may cite locations in Portugal, France and Italy, where cases of dengue and Chikungunya have already been recorded, the United States with cases of dengue fever and Zika virus, and Brazil, where dengue has been endemic for many years (Wang et al. 2017; dos Santos et al. 2018; Amaku et al. 2016; Massad et al. 2008; Burattini et al. 2016; Iggidr et al. 2017).

Dengue is currently one of the human viral diseases with the highest number of cases, it is transmitted through the bite of female mosquitoes of the genus *Aedes*, which are an arbovirus of the family Flaviviridae, genus *Flavivirus*. It is estimated to be endemic in more than 100 countries, and approximately half of the world's population is at risk of contracting the disease (Liu-Helmersson et al. 2016; Kraemer et al. 2015; Bhatt et al. 2013; Rodriguez-Barraquer et al. 2011). The usual control measures are related to mosquitoes' population with the use of insecticides in addition to public awareness campaigns, also the *Wolbachia* bacteria has been investigated as a possibility to prevent the vector from transmitting the virus (King et al. 2018) and currently some vaccines have been tested or are in testing phase (Precioso et al. 2015; Boccia et al. 2014).

Mathematical models applied to describe indirectly transmitted infectious diseases must couple the dynamics of hosts and vectors, whose parameters have different time scales, mosquitoes have a life cycle of days while the human life cycle is years. Studies with spatial networks, or meta-populations, provide a way to understand the interactions between individuals in different scales, being a powerful tool to understand the characteristics of transmission in communities, regions and countries incorporating spatial heterogeneity (Massad et al. 2008; Barmak et al. 2011; Iggidr et al. 2017; Kiss et al. 2006; Newman 2003; Brockmann et al. 2009). If the goal is to fit the model to real data, it is necessary to deal with missing information, in particular for the mosquitoes' population, besides having to take into account the different time scales of vectors and hosts (Rocha et al. 2013; Souza 2014).

In this work, we consider a host-vector disease compartmental model that divides the host population into susceptible $S$, infected $I$ and recovered $R$, coupled with susceptible $S_m$ and infected mosquitoes $I_m$. This model depends on parameters such as the mosquitoes mortality rate and the total vector population, which are very difficult to measure. From this model we do the time-scale separation of hosts and vectors. As a consequence, the order of the model is reduced as long as the mosquitoes equations do not appear explicitly in the model and only one of the remaining parameters will depend on the mosquitoes mortality rate. Finally, we incorporate human spatial movements, considering mobility between cities two to two. We adjust this model to dengue incidence data from cities which were chosen based on previous evidence of human mobility related to disease spread (dos Santos et al. 2018). Thereby, our main purpose is to show that this model provides a good approximation of the number of infected individuals when fitting the nonlinear incidence rate equations to dengue incidence data, as well as the possibility of obtaining parameters simulating human movement between two cities.

First, our approach will be deterministic. Secondly, being more precise, the goal is to consider the effects of the spatial dynamics into the Ross–Macdonald models and use it to fit the real data. This can be done either by a continuous space domain, which in turn will give us partial differential equations, local or non-local, or consider discrete networks in space, which will provide a system of ordinary differential equations (ODE). There are advantages and disadvantages to both approaches. From the mathematical point of view, there are several theoretical challenges in the continuous model, in particular if non-local operators are considered, even if one proves that the second approach can be viewed as an approximation of the first and that the dynamics must somehow converge. The second approach can more easily be used to fit the real data, in view of it is always discrete in nature. Since, in this work, we are interested in concrete data and fit the dynamics, we will concentrate on the second model. For the continuous model, one can refer to Ducrot et al. (2017); Pereira et al. (2020) where similar approaches were considered, and rigorous results were obtained.

The paper is organized as follows. First, we specify the local dynamics that will describe the disease transmission in each city, we also identify the small parameter that will be used. Next, we set up the network dynamic, introducing a diffusion operator. With these two ingredients, for completeness, we show a formal expansion that reflects the general ODE singular perturbation results shown in details in Pereira et al. (2020). Finally, we can estimate our parameters using a network found to represent the initial spread of the disease in the State of Rio de Janeiro, Brazil, and present our results.

## 2 Setting the Model

We consider a model, named SIRS$_m I_m$, following the frequency-dependent structure of the well-known Ross–Macdonald models. The total host population $N_h$ is divided into susceptible $S$, infected $I$ and recovered $R$ and it is coupled with the compartments of susceptible $S_m$ and infected $I_m$ mosquitoes with total population given by $N_m$. The interaction dynamics between the compartments is described through the system of ordinary differential equations (ODEs):

$$\begin{aligned} \mathrm{d}S/\mathrm{d}t &= \mu_h(N_h - S) - \beta S I_m/N_m \\ \mathrm{d}I/\mathrm{d}t &= \beta S I_m/N_m - (\gamma + \mu_h)I \\ \mathrm{d}R/\mathrm{d}t &= \gamma I - \mu_h R \\ \mathrm{d}S_m/\mathrm{d}t &= \mu_m(N_m - S_m) - \Omega S_m I/N_h \\ \mathrm{d}I_m/\mathrm{d}t &= \Omega S_m I/N_h - \mu_m I_m \end{aligned} \tag{1}$$

In this model, $\beta$ denotes the average number of contacts enough to receive infection which hosts make with mosquitoes per unit time. Precisely, $\beta$ is a product of two factors, the biting rate, and the probability that a bite transmits infection from vector to human. In this way, a susceptible human $S$, receives $\beta$ effective mosquitoes bites, of which a fraction $I_m/N_m$ is with an infected mosquito so, the number of new infected humans, in unit time, is $\beta S I_m/N_m$. Reciprocally, a susceptible mosquito $S_m$ makes $\Omega$ effective contacts with humans, where a fraction $I/N_h$ is with and infected individual. The number of new infected mosquitoes, in unit time, is $\Omega S_m I/N_h$ (Brauer et al.

2016). The parameter $\gamma$ is the human recovery rate, and the parameters $\mu_h$ and $\mu_m$ are the birth/mortality rate, respectively, of humans and mosquitoes; both are calculated by the inverse of life expectancy.

As we will work with a short period of time (less than one year), it is possible to suppose that populations remain constant; that is, birth and mortality rates are equal, so $N_h(t) = S(t) + I(t) + R(t)$ and $N_m(t) = S_m(t) + I_m(t)$. Consequently, $R(t) = N_h(t) - S(t) - I(t)$ and $S_m(t) = N_m(t) - I_m(t)$, then we can work with the equivalent reduced system:

$$\begin{aligned} \mathrm{d}S/\mathrm{d}t &= \mu_h(N_h - S) - \beta S I_m/N_m \\ \mathrm{d}I/\mathrm{d}t &= \beta S I_m/N_m - (\gamma + \mu_h)I \\ \mathrm{d}I_m/\mathrm{d}t &= \Omega(N_m - I_m)I/N_h - \mu_m I_m \end{aligned} \tag{2}$$

Considering that the life expectancy of an adult female mosquito is about 10 days (Liu-Helmersson et al. 2016), and a human life expectancy of 73 years (2010 Brazilian Census), the value of $\mu_m = 1/10$ (days) is bigger than the corresponding parameter of humans $\mu_h = 1/(365 \times 73)$ (days) (Rocha et al. 2013). To describe the time-scale separation, we add the singular term $1/\varepsilon$ as done in Rocha et al. (2013); Souza (2014) and Pereira et al. (2020). Defining $\mu_m = \overline{\mu_m}/\varepsilon$ and $\Omega := \overline{\Omega}/\varepsilon$, with $\overline{\mu_m}$ in the time scale of $\mu_h$, and setting up $\overline{\mu_m} := \mu_h$, we obtain $\varepsilon = \mu_h/\mu_m$, then replacing these parameters in (2), follows that

$$\begin{aligned} \mathrm{d}S/\mathrm{d}t &= \mu_h(N_h - S) - \beta S I_m/N_m \\ \mathrm{d}I/\mathrm{d}t &= \beta S I_m/N_m - (\gamma + \mu_h)I \\ \varepsilon \mathrm{d}I_m/dt &= \overline{\Omega}(N_m - I_m)I/N_h - \overline{\mu_m} I_m \end{aligned} \tag{3}$$

As in Rocha et al. (2013); Pereira et al. (2020), we establish a system where the vector population dynamics is much faster than hosts one as $\varepsilon \approx 0$. At $\varepsilon = 0$, (see (Pereira et al. 2020) for convergence), $I_m(t)$ can be obtained as a function of $I(t)$ at any time $t$:

$$I_m(t) = \frac{\overline{\Omega} I(t) N_m}{\overline{\Omega} I(t) + \overline{\mu_m} N_h} \tag{4}$$

Replacing (4) into the equations of System (3), give us a new equivalent system with a nonlinear incidence rate without the mosquitoes equation:

$$\begin{aligned} \frac{\mathrm{d}S}{\mathrm{d}t} &= \mu_h(N_h - S) - \frac{\beta \overline{\Omega} I S}{\overline{\Omega} I + \overline{\mu_m} N_h} \\ \frac{\mathrm{d}I}{\mathrm{d}t} &= \frac{\beta \overline{\Omega} I S}{\overline{\Omega} I + \overline{\mu_m} N_h} - (\gamma + \mu_h) I \end{aligned} \tag{5}$$

### 2.1 Spatial Dynamics

The SIRS$_m I_m$ model characterizes the dynamics of a disease within a population. If the purpose is to describe its transmission dynamics more realistically, it is necessary

to consider a mobility network that includes interaction between populations (Iggidr et al. 2017; Newman 2003). Let $N_{hr}$ be the total human population that is registered in node $r = 1, 2, \ldots, M$, so the disease dynamics in each location is described by the $S_r I_r R_r S_{m_r} I_{m_r}$ model. The parameter $d_{rs}$ corresponds to the mobility rate from the population $r$ to $s$ per unit time (Iggidr et al. 2017).

To include spatial dynamics in model (1), we must consider the inflow and outflow of humans in each compartment. In order to avoid adding more complexity to the model, we consider two hypotheses. The first one, is that human movement is the same in all classes. This is reasonable since it is estimated that only 25% of the infected manifests any level of the disease severity, the others 75% are asymptomatic or with mild infections and keep moving around carrying the virus (Bhatt et al. 2013). This contributes to transmit the virus to susceptible mosquitoes from other locations. Second, we do not consider the movement of vectors performed by humans, and as mosquitoes do not move large distances (Bomfim et al. 2020), their respective compartments remain unchanged. The system of equations representing human mobility between cities $r$ and $s$, $r \neq s$, is given by:

$$\begin{aligned}
\mathrm{d}S_r/\mathrm{d}t &= \mu_h(N_{\mathrm{hr}} - S_r) - \beta_r S_r I_{m_r}/N_{\mathrm{mr}} + \sum_{r\neq s}(\mathrm{d}_{\mathrm{sr}} S_s - d_{\mathrm{rs}} S_r)\\
\mathrm{d}I_r/\mathrm{d}t &= \beta_r S_r I_{m_r}/N_{\mathrm{mr}} - (\gamma + \mu_h) I_r + \sum_{r\neq s}(d_{\mathrm{sr}} I_s - \mathrm{d}_{\mathrm{rs}} I_r)\\
\mathrm{d}R_r/\mathrm{d}t &= \gamma I_r - \mu_h R_r + \sum_{r\neq s}(\mathrm{d}_{\mathrm{sr}} R_s - \mathrm{d}_{\mathrm{rs}} R_r)\\
\mathrm{d}S_{m_r}/\mathrm{d}t &= \mu_{mr}(N_{m_r} - S_{m_r}) - \Omega_r S_{m_r} I_r/N_{\mathrm{hr}}\\
\mathrm{d}I_{m_r}/\mathrm{d}t &= \Omega_r S_{m_r} I_r/N_{\mathrm{hr}} - \mu_{mr} I_{m_r}
\end{aligned} \tag{6}$$

with initial conditions $S_r(0) \geq 0$, $I_r(0) \geq 0$, $R_r(0) \geq 0$, $S_{m_r}(0) \geq 0$, $I_{m_r}(0) \geq 0$. Here, we suppose that parameters are different for each location except the host birth/mortality rate $\mu_h$ and the recovery rate $\gamma$. The total host population in each area is given by $N_{\mathrm{hr}} = S_r + I_r + R_r$, so

$$\begin{aligned}
\mathrm{d}N_{\mathrm{hr}}/\mathrm{d}t &= \mathrm{d}S_r/\mathrm{d}t + \mathrm{d}I_r/\mathrm{d}t + \mathrm{d}R_r/\mathrm{d}t\\
&= \mu_h(N_{\mathrm{hr}} - S_r - I_r - R_r) + \sum_{r\neq s}(\mathrm{d}_{\mathrm{sr}}(S_s + I_s + R_s) - \mathrm{d}_{\mathrm{rs}}(S_r + I_r + R_r))\\
&= \sum_{r\neq s}(\mathrm{d}_{\mathrm{sr}} N_{\mathrm{hs}} - \mathrm{d}_{\mathrm{rs}} N_{\mathrm{hr}})
\end{aligned}$$

Similarly as done to obtain (5) and considering the spatial dynamics in (6), we accomplish the $S_r I_r$ model:

$$\frac{\mathrm{d}S_r}{\mathrm{d}t} = \mu_h(N_{\mathrm{hr}} - S_r) - \frac{\beta_r \overline{\Omega_r} I_r S_r}{\overline{\Omega_r} I_r + \overline{\mu_{mr}} N_{\mathrm{hr}}} + \sum_{r\neq s}(\mathrm{d}_{\mathrm{sr}} S_s - \mathrm{d}_{\mathrm{rs}} S_r)$$

$$\frac{\mathrm{d}I_r}{\mathrm{d}t} = \frac{\beta_r \overline{\Omega_r} I_r S_r}{\overline{\Omega_r} I_r + \overline{\mu_{mr}} N_{hr}} - (\gamma + \mu_h) I_r + \sum_{r \neq s} (\mathrm{d}_{\mathrm{sr}} I_s - \mathrm{d}_{\mathrm{rs}} I_r) \tag{7}$$

This is a nonlinear incidence rate system with populations interaction. The dynamics of this kind of modified equations was already studied for some authors. Souza (2014) showed that for the SIRSI model with fast vector dynamics, the equilibria are preserved by the asymptotic approximation, and the global stability dynamics is consistent with the global stability dynamics of the full model. Hethcote and Van den Driessche (1991) analyzed the SEIRS epidemiological model with nonlinear incidence rates. They used the general form $\beta g(I)S$ where $g(I) = (I^p)/(1 + \alpha I^q)$, $p, q > 0, \alpha \geq 0$ and their results showed that for $p = q = 1$ the usual epidemic patterns holds; that is, below the threshold ($= 1$), the disease dies out and above the thresholds the disease approach to endemic equilibrium independent of $\alpha$.

Besides the nonlinear incidence rate, our system includes human mobility, so the proof of the global stability is non-trivial. However, we show through numerical simulations that the number of infected individuals persists at a positive level for our estimated parameters; that is, when $R_0 > 1$, the disease tends to an endemic state (see Appendix 6).

### 2.2 Asymptotic Expansion

Here, a power series expansion is used to analyze the asymptotic behavior with respect to parameter $\varepsilon > 0$ of the perturbed System (3) with spatial dynamics as in (6). In order to do that, let $\mathbf{S}$, $\mathbf{I}$ and $\mathbf{I_m}$ be vectorial functions whose coordinates are denoted, respectively, by $S_r$, $I_r$ and $I_{mr}$ for $r = 1, 2, ..., M$. We consider the following singular perturbed system of ODEs:

$$\begin{aligned}
\mathrm{d}S_r/\mathrm{d}t &= \mu_h(N_{h_r} - S_r) - \beta_r S_r I_{m_r}/N_{m_r} + \sum_{r \neq s} (\mathrm{d}_{\mathrm{sr}} S_s - \mathrm{d}_{\mathrm{rs}} S_r) \\
\mathrm{d}I_r/\mathrm{d}t &= \beta_r S_r I_{m_r}/N_{m_r} - (\gamma + \mu_h) I_r + \sum_{r \neq s} (\mathrm{d}_{\mathrm{sr}} I_s - \mathrm{d}_{\mathrm{rs}} I_r) \\
\varepsilon \mathrm{d}I_{m_r}/\mathrm{d}t &= \overline{\Omega_r}(N_{m_r} - I_{m_r}) I_r/N_{h_r} - \overline{\mu_{mr}} I_{m_r}
\end{aligned} \tag{8}$$

We expand the solutions with respect to the small parameter $\varepsilon$ assuming that the vectorial functions $\mathbf{S}$, $\mathbf{I}$ and $\mathbf{I_m}$ given by (8) satisfy

$$\mathbf{S} = \mathbf{S}_0 + \varepsilon \mathbf{S}_1 + \varepsilon^2 \mathbf{S}_2 + \cdots \qquad \mathbf{I} = \mathbf{I}_0 + \varepsilon \mathbf{I}_1 + \varepsilon^2 \mathbf{I}_2 + \cdots$$

and

$$\mathbf{I_m} = \mathbf{I_{m0}} + \varepsilon \mathbf{I_{m1}} + \varepsilon^2 \mathbf{I_{m2}} \ldots$$

Thus, the time derivatives themselves set

$$\frac{\mathrm{d}\mathbf{S}}{\mathrm{d}t} = \frac{\mathrm{d}\mathbf{S}_0}{\mathrm{d}t} + \varepsilon \frac{\mathrm{d}\mathbf{S}_1}{\mathrm{d}t} + \cdots \qquad \frac{\mathrm{d}\mathbf{I}}{\mathrm{d}t} = \frac{\mathrm{d}\mathbf{I}_0}{\mathrm{d}t} + \varepsilon \frac{\mathrm{d}\mathbf{I}_1}{\mathrm{d}t} + \cdots$$

and

$$\frac{\mathrm{d}\mathbf{I_m}}{\mathrm{d}t} = \frac{\mathrm{d}\mathbf{I_{m0}}}{\mathrm{d}t} + \varepsilon \frac{\mathrm{d}\mathbf{I_{m1}}}{\mathrm{d}t} + \cdots$$

If we plug these expressions in System (8), after some computations, the following equations are obtained at $\varepsilon = 0$:

$$\begin{aligned}
\mathrm{d}S_{r0}/\mathrm{d}t &= \left[ \mu_h(N_{hr} - S_{r0}) - \beta_r S_{r0} I_{mr0}/N_{mr} + \sum_{r \neq s} (\mathrm{d_{sr}} S_{s0} - \mathrm{d_{rs}} S_{r0}) \right] \\
\mathrm{d}I_{r0}/\mathrm{d}t &= \left[ \beta_r S_{r0} I_{mr0}/N_{mr} - (\gamma + \mu_h) I_{r0} + \sum_{r \neq s} (d_{\mathrm{sr}} I_{s0} - \mathrm{d_{rs}} I_{r0}) \right] \\
0 &= \left[ \overline{\Omega_r}(N_{mr} - I_{mr0}) I_{r0}/N_{h_r} - \overline{\mu_{mr}} I_{mr0} \right].
\end{aligned}$$

Hence, we get as in (4) that

$$I_{m_{r_0}} = \frac{\overline{\Omega_r} I_{r_0} N_{m_r}}{\overline{\Omega_r} I_{r_0} + \overline{\mu_{mr}} N_{h_r}}$$

and then, we deduce the reduced system

$$\begin{aligned}
\frac{\mathrm{d}S_{r0}}{\mathrm{d}t} &= \mu_h(N_{h_r} - S_{r0}) - \frac{\beta_r \overline{\Omega_r} I_{r0} S_{r0}}{\overline{\Omega_r} I_{r_0} + \overline{\mu_{mr}} N_{h_r}} + \sum_{r \neq s} (\mathrm{d_{sr}} S_{s0} - \mathrm{d_{rs}} S_{r0}) \\
\frac{\mathrm{d}I_{r0}}{\mathrm{d}t} &= \frac{\beta_r \overline{\Omega_r} I_{r0} S_{r0}}{\overline{\Omega_r} I_{r_0} + \overline{\mu_{mr}} N_{h_r}} - (\gamma + \mu_h) I_{r0} + \sum_{r \neq s} (d_{\mathrm{sr}} I_{s0} - \mathrm{d_{rs}} I_{r0})
\end{aligned}$$

with initial condition $S_{r0}(0) \geq 0$ and $I_{r0}(0) \geq 0$ as in (7) and without the mosquitoes equations. We conclude that the solutions $\mathbf{S}$ and $\mathbf{I}$ of System (8) can be approximated by solutions of the limit System (7). Indeed, it follows from our previous work (Pereira et al. 2020) (see also (Rocha et al. 2013; Souza 2014) and [ Hartmann (2008), Theorem 4.4]) that the convergence is uniform in finite time with order $O(\varepsilon)$.

## 3 Parameter Estimation

We have System (7) with nonlinear incidence rate, which does not depend on the mosquitoes equations and coupled with spatial dynamics. Estimating parameters is a challenging task, especially in the case of fitting the model for two or more time series simultaneously, and also taking into account that the parameters need to have real meaning for the disease being applied.

For deterministic models, the fitting consists in finding the model trajectory that best represent the data. When estimating one or two parameters, it is possible to search in all range of the parameters for the values that provides the optimum global. However, when dealing with many parameters, the search will be computationally expensive and not viable.

In this work, we employed the **pomp** package implemented in R language described in King et al. (2015), in order to obtain the values for: $\beta_r$, $\overline{\Omega_r}$, $\overline{\mu_{mr}}$, $d_{rs}$, $\gamma$ and the initial conditions of each location $S_r(0)$ and $I_r(0)$. We used the algorithm of the section related to *Fitting deterministic dynamical epidemiological models to data*, which can be found at King (2022). It was adapted to fit the solution $I_r$ from the $S_r I_r$ model to dengue incidence data of Brazilian cities which present evidence of human mobility acting as a virus spreading factor (dos Santos et al. 2018).

The adjustment is done using the least squares method. First, we set up a function to calculate the sum of the squared errors (King 2022), which is determined by the difference between the solutions $I_r$ obtained with the deterministic model and dengue incidence data from each respective city. This is done for two time series simultaneously. After setting up the error function which is the objective function, we define our global parameters and the parameters that need to be estimated. To each parameter and variable can be given a lower and/or upper bound, then it is necessary to start with an initial value which satisfies the constraints and from this point, the optimization algorithm uses the function values and gradients to search the parameter space for the value that minimizes the objective function (King 2022). As it is an ill-posed problem, we run many simulations with different initial conditions. Then, we selected the one which returns the minimum sum of the squared errors.

Considering that there are errors when the incidence cases are recorded, we can suppose these errors, in each observation, are normally distributed, and then it is possible to build an interval of variation for the observations. Here, it would be desirable to build a profile likelihood for each parameter by fixing the values obtained with the optimization algorithm and then varying one parameter per time but dealing with many parameters it becomes not reasonable. When using the normal distribution, the mean is the model prediction and the variance can be estimated or defined (King 2022).

The model with time-scale separation and considering mobility among two cities is given by:

$$
\begin{aligned}
\mathrm{d}S_1/\mathrm{d}t &= \mu_h(N_{h1} - S_1) - \frac{\beta_1\overline{\Omega_1}I_1S_1}{\overline{\Omega_1}I_1 + \overline{\mu_{m1}}N_{h1}} + \mathrm{d}_{21}S_2 - \mathrm{d}_{12}S_1 \\
\mathrm{d}I_1/\mathrm{d}t &= \frac{\beta_1\overline{\Omega_1}I_1S_1}{\overline{\Omega_1}I_1 + \overline{\mu_{m1}}N_{h1}} - (\gamma + \mu_h)I_1 + \mathrm{d}_{21}I_2 - \mathrm{d}_{12}I_1 \\
\mathrm{d}S_2/\mathrm{d}t &= \mu_h(N_{h2} - S_2) - \frac{\beta_2\overline{\Omega_2}I_2S_2}{\overline{\Omega_2}I_2 + \overline{\mu_{m2}}N_{h2}} + \mathrm{d}_{12}S_1 - \mathrm{d}_{21}S_2 \\
\mathrm{d}I_2/\mathrm{d}t &= \frac{\beta_2\overline{\Omega_2}I_2S_2}{\overline{\Omega_2}I_2 + \overline{\mu_{m2}}N_{h2}} - (\gamma + \mu_h)I_2 + \mathrm{d}_{12}I_1 - \mathrm{d}_{21}I_2
\end{aligned}
\tag{9}
$$

where

$$\begin{aligned} \mathrm{d}N_{h1}/\mathrm{d}t &= d_{21}N_{h2} - d_{12}N_{h1} \\ \mathrm{d}N_{h2}/\mathrm{d}t &= d_{12}N_{h1} - d_{21}N_{h2} \end{aligned}$$

For System (9), we calculate the basic reproduction number $R_0$ through the next generation matrix method (van den Driessche 2017). For vector-borne diseases, the value of $R_0$ means the number of new infectives per infective, per generation. The compartments with infected are $I_1$ and $I_2$. In order to work with the disease free equilibrium $(S_1, I_1, S_2, I_2) = (N_{h_1}, 0, N_{h_2}, 0)$, it is necessary to consider the restriction $d_{21} = d_{12}(N_{h1}/N_{h2})$, so the populations remains constant even considering spatial dynamics. See that such condition is reasonable for short data periods.

The matrix $\mathbf{F}$ containing the appearance rates of new infections, and the matrix $\mathbf{V}$ with the other transitions among the compartments are, respectively:

$$\mathbf{F} = \begin{bmatrix} \frac{\beta_1\overline{\Omega_1}}{\overline{\mu_{m_1}}} & d_{21} \\ d_{12} & \frac{\beta_2\overline{\Omega_2}}{\overline{\mu_{m_2}}} \end{bmatrix} \; and \; \mathbf{V} = \begin{bmatrix} (\gamma + \mu_h + d_{12}) & 0 \\ 0 & \gamma + \mu_h + d_{21} \end{bmatrix}. \tag{10}$$

The $R_0 = \rho(\mathbf{F}\mathbf{V}^{-1})$, is given by:

$$R_0 = \frac{\lambda_2\gamma_{12} + \lambda_1\gamma_{21}}{2\gamma_{12}\gamma_{21}} + \frac{\sqrt{(\lambda_2\gamma_{12} + \lambda_1\gamma_{21})^2 - 4(\gamma_{12}\gamma_{21})(\lambda_1\lambda_2 - d_{12}d_{21})}}{2\gamma_{12}\gamma_{21}} \tag{11}$$

where $\lambda_i = \beta_i\overline{\Omega_i}/\overline{\mu_{mi}}$ and $\gamma_{ij} = \gamma + \mu_h + d_{ij}, i, j = 1, 2, i \neq j$.

In Appendix 6.1, we also show the $R_0$ expression for System (1) without human mobility.

### 3.1 Data

We work with dengue data obtained from Brazil's Information System for Notifiable Diseases (SINAN) (da Saúde/SVS DATASUS 2020). Dengue time series only provide the amount of humans infected weekly. The year 2008 was chosen for results simulation due to the high number of reported cases in Rio de Janeiro state and by the incidence to present a well-defined qualitative behavior. We only consider the period from the 1st week to the 35th week of 2008. The number of reported cases per week (incidence per week) in Rio de Janeiro city, Duque de Caxias, Itaboraí, Niterói and Nova Iguaçu is shown in Fig. 1. It will be used to fit the $I_r$ solutions from the Model (9).

These cities were chosen among all others due to the evidence of human mobility acting as a virus spread factor as discussed in dos Santos et al. (2018), which used the ideas of Saba et al. (2014); Brockmann and Helbing (2013) to identify an effective network that explains the epidemic in Rio de Janeiro. Notifications are made in basic health units and are recorded manually, so there may be errors when recording data computationally, another discrepancy may be caused by notifications accumulated in weeks with holidays and only recorded in the following week.

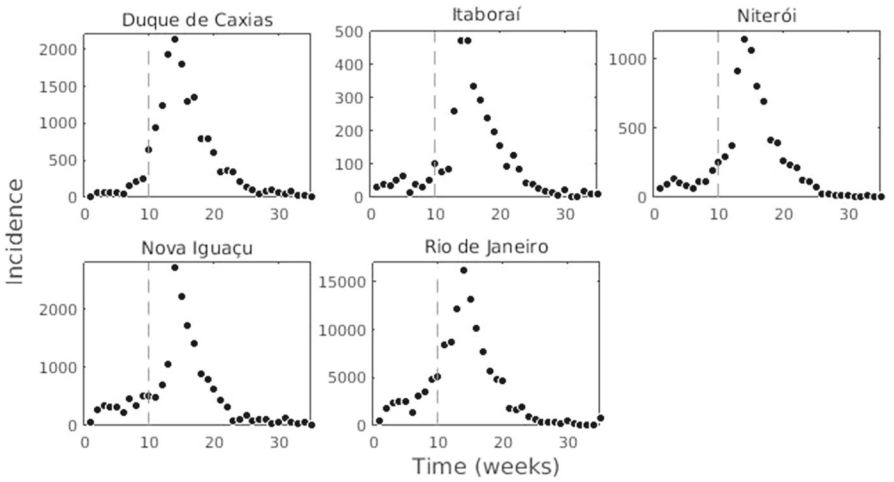


**Fig. 1** Incidence of dengue in Duque de Caxias, Itaboraí, Niterói, Nova Iguaçu and Rio de Janeiro, in the period from the 1st week of 2008 to the 35th week of 2008

**Table 1** The total population size of each city $N_{h_i}$. Information from the 2010 Brazilian Census

| Cities | Population $N_{h_i}$ |
|---|---|
| Duque de Caxias | 855048 |
| Itaboraí | 218008 |
| Niterói | 487562 |
| Nova Iguaçu | 796257 |
| Rio de Janeiro | 6320446 |

The fixed parameters are the total population of each city presented in Table 1, and the birth/mortality rate of humans, calculate as the inverse of the life expectancy (73 years for Brazil in 2010). The second is considered the same for all cities, and both were obtained from the 2010 Brazilian Census. The other parameters need to be estimated.

## 4 Results

Regarding the initial values of the parameters, we will consider that the initial susceptible population is 98% of the total population of each city, $S_r(0) = 0.98 \times N_{hr}$ and $I_r(0)$ ranges from 1 to 10. The human recovery rate $\gamma$ is initially one week since the data are incidence per week. The mobility parameter $d_{12}$ start with the value $d_{12} = 0.0001$, while its result can ranges from 0 to 0.02, restriction imposed due to the population of Rio de Janeiro being very dense compared to the other cities, so $d_{21}$ is calculated by $d_{21} = d_{12}(N_{h1}/N_{h2})$.

As a consequence of considering System (9) with time scale separation, we do not have vectors' equations, and recalling that by definition: $\overline{\Omega_r} = \varepsilon\Omega_r$ and $\overline{\mu_m} = \varepsilon\mu_m$,

**Table 2** Parameters estimated.

| Pairs of cities | Parameters (weeks) | | | | | | | |
|---|---|---|---|---|---|---|---|---|
| | $\beta_r$ | $\overline{\Omega_r}$ | $\overline{\mu_{mr}}$ | $\gamma$ | $d_{rs}$ | $S_r$ | $I_r$ | $R_0$ |
| Rio de Janeiro[1] Niterói[2] | 3.708568 2.384147 | 3.765754 2.503814 | 1.723850 0.7356344 | 7.388 | 0.0200 0.2593 | 6194037.0 477810.8 | 12.87 15.15 | 1.096 |
| Rio de Janeiro[1] Duque de Caxias[2] | 2.552321 2.742951 | 3.235730 2.749064 | 0.9830482 0.9011295 | 7.640 | 0.0200 0.1478 | 6194037.0 837947.0 | 10.0 10.0 | 1.099 |
| Rio de Janeiro[1] Nova Iguaçu[2] | 2.342745 1.916802 | 2.554152 2.022191 | 0.7940922 0.5124775 | 6.854 | 0.0200 0.1588 | 6194037.0 780331.9 | 19.75 21.31 | 1.099 |
| Duque de Caxias[1] Nova Iguaçu[2] | 3.064016 3.074946 | 3.236830 3.223660 | 1.169814 1.172522 | 7.678 | 0.01406 0.01510 | 837947.0 780331.9 | 1.10 1.07 | 1.103 |
| Niterói[1] Itaboraí[2] | 3.812321 3.038121 | 4.091723 3.034493 | 1.856236 1.102519 | 7.674 | 0.01231 0.02752 | 477810.8 213647.8 | 1.16 0.54 | 1.094 |

In the first column are shown the pairs of cities, numbered 1 and 2, and in the following columns, the respective parameter values. The ones related to mobility are $d_{12}$ and $d_{21}$, where only $d_{12}$ is estimated and it represents the proportion of the population leaving city 1 and going to city 2 and $d_{21} = d_{12}(N_{h_1}/N_{h_2})$ is the opposite. Finally, the $R_0$ value is calculated using the expression (11)

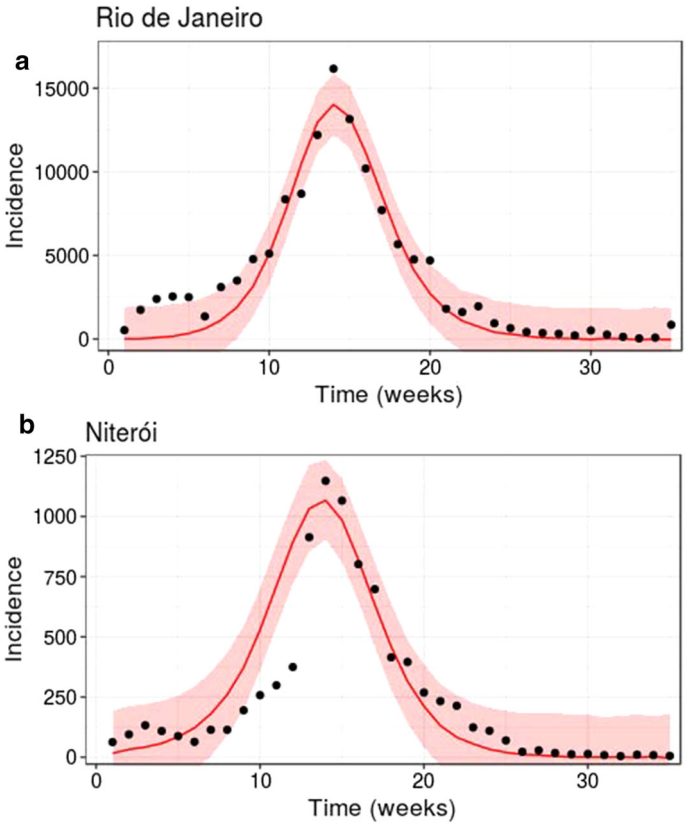


**Fig. 2** Result of fitting equations $I_1$ and $I_2$ from Model 9 to dengue incidence data from Rio de Janeiro and Niterói, respectively, according to the parameters of Table 2. In black dots, is the incidence per week, the solid lines (in red) show the results obtained from the model and the region (filled with red) is the 95% confidence interval (CI) for the variation of the observations (color figure online)

from the nonlinear incidence terms in (9), result that

$$\frac{\beta_r(\varepsilon\Omega_r)I_rS_r}{(\varepsilon\Omega_r)I_r+(\varepsilon\mu_m)N_{hr}}=\frac{\beta_r\Omega_rI_rS_r}{\Omega_rI_r+\mu_{mr}N_{hr}}.$$

In fact, only $\mu_{mr}$ is an intrinsic parameter of mosquitoes present in the system, being necessary to make an initial assumption for its value. In addition, it is consistent to suppose this mortality rate may vary in different regions, as there may be distinct strategies to combat vectors in each city. Let us consider initially a life expectancy of 10 days, so $\mu_{mr} = 7/10$ (weeks) Liu-Helmersson et al. (2016). Finally, we scan for the initial values of the rates $\beta_r$ and $\overline{\Omega_r}$ in the range $[0.5, 10.0]$ and then return the fitting that results in the smallest quadratic error.

These are initial guesses for the parameter's values, the result achieved may be outside these ranges. In the optimization algorithm we only define the upper limit for $d_{12}$, and the lower limit as 0 for all parameters. Notice, that in each respective

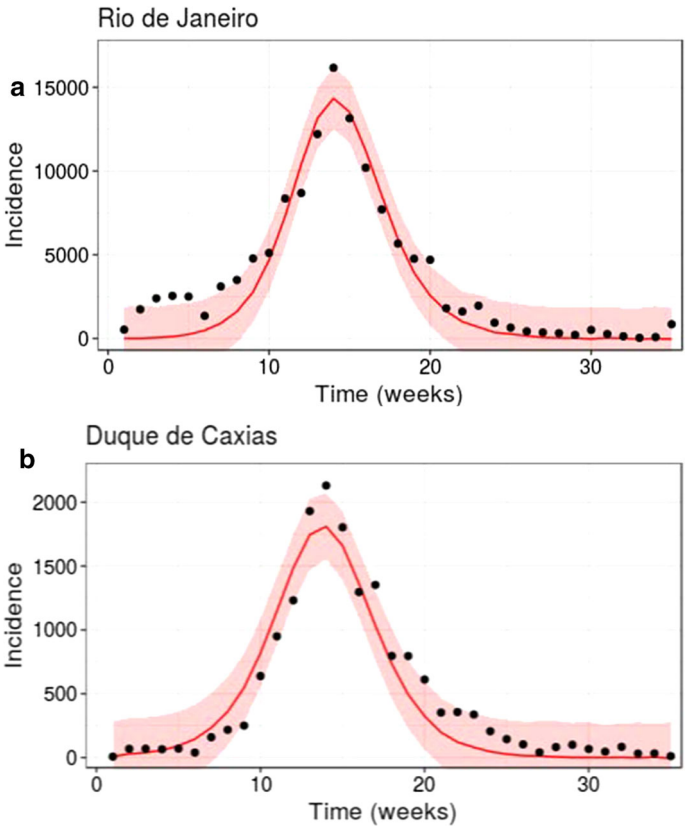


**Fig. 3** Result of fitting equations $I_1$ and $I_2$ from Model 9 to dengue incidence data from Rio de Janeiro and Duque de Caxias, respectively, according to the parameters of Table 2. Black dots show the incidence per week, the solid lines (in red) show the results obtained from the model, and the region (filled with red) is the 95% confidence interval (CI) for the variation of the observations (color figure online)

simulation, the value of 12 parameters are estimated. It is not computationally feasible to scan a range for all initial values, so it is only done for $I_r(0)$, $\beta_r$ and $\overline{\Omega_r}$.

The results obtained are presented in Table 2 for each pair of cities. In the sequence, the figures containing the respective adjustments. From Figs. 2, 3, 4, 5 and 6, the incidence is the number of new cases recorded per week (black dots), the solid lines (in red) are the average of infected individuals obtained with the deterministic model and the region (filled with red) is the 95% confidence interval (CI) for the variation of the observations.

## 5 Discussion

From the SIRS$_m I_m$ vector-host model, we made a separation of time scales, and the system was reduced to an equivalent one with nonlinear incidence rate independent of the mosquitoes' equations. Then, we added human spatial dynamics to this new

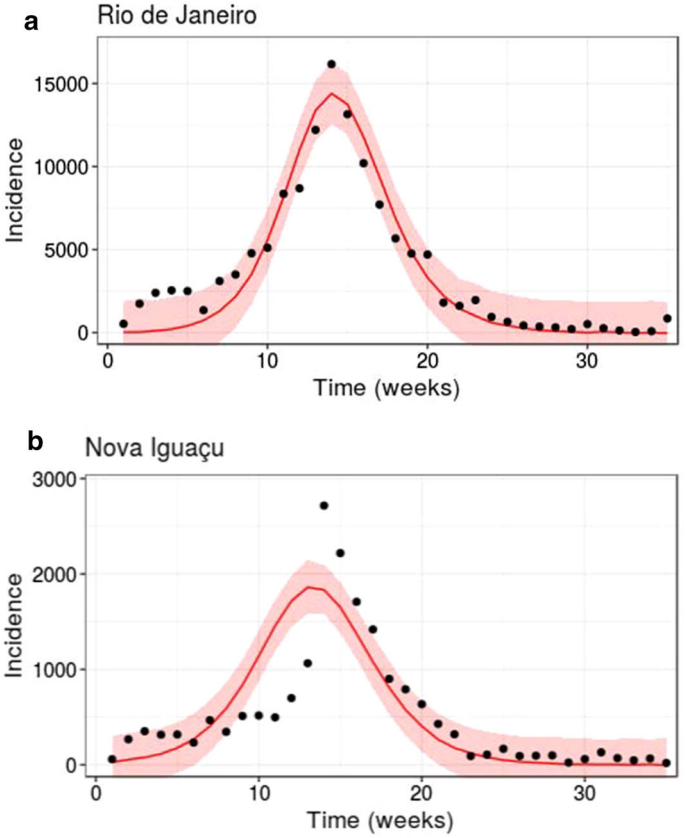


**Fig. 4** Result of fitting equations $I_1$ and $I_2$ from Model 9 to dengue incidence data from Rio de Janeiro and Nova Iguaçu, respectively, according to the parameters of Table 2. Black dots show the incidence per week, the solid lines (in red) show the results obtained from the model, and the region (filled with red) is the 95% confidence interval (CI) for the variation of the observations (color figure online)

system named $S_r I_r$. The parameters present in the modified equations depend on the respective parameters of humans, with only one intrinsic of mosquitoes ($\mu_m$), whereas the full $SIRS_m I_m$ model contains two parameters related to vectors ($\mu_m$ and $N_m$), which makes it more difficult to fit the model to data due to the lack of available information about mosquitoes.

This reduction contributes to a better estimation of parameters, as long as the mosquitoes mortality rate is easier to be estimated than its population size. The first one is possible to be measured clinically in laboratories, and the second, in addition to not being possible to have a reliable measurement, its proportion related to the host population, may vary from city to city.

We made some considerations about the initial value of the parameters in order to apply an algorithm to fit the model to dengue data of some pairs of cities in Rio de Janeiro state. As it is possible to see from the incidence data (Fig. 1), Rio de Janeiro and Niterói are the first cities to present a consecutive increase in the number of cases

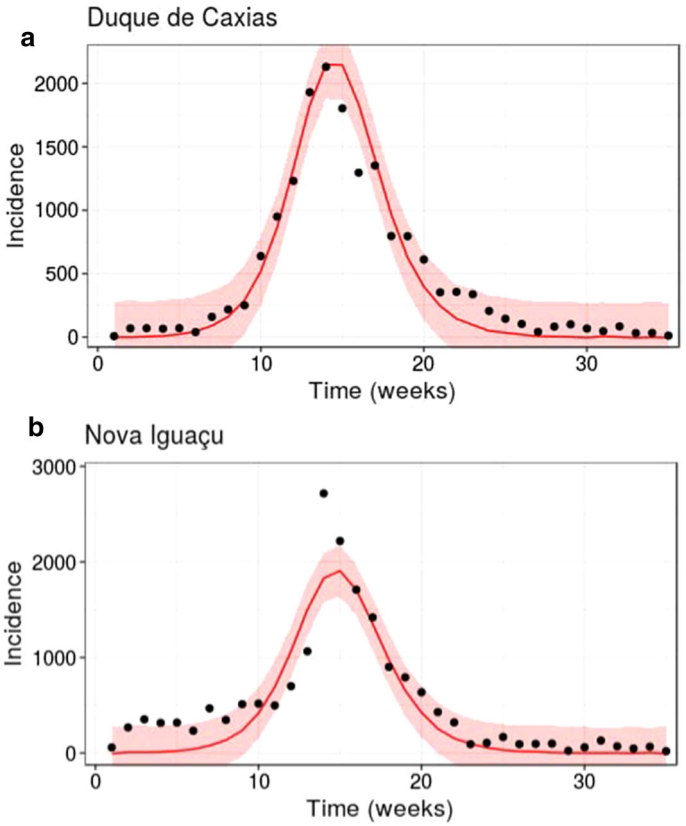


**Fig. 5** Result of fitting equations $I_1$ and $I_2$ from Model 9 to dengue incidence data from Duque de Caxias and Nova Iguaçu, respectively, according to the parameters of Table 2. Black dots show the incidence per week, the solid lines (in red) show the results obtained from the model, and the region (filled with red) is the 95% confidence interval (CI) for the variation of the observations (color figure online)

before the 10th epidemiological week, while to the other cities the rise occurred a bit later. These two locations work as focus of the disease, and according to the real distance between them, it makes sense that the flow of people occurs among Rio de Janeiro and Niterói; Rio de Janeiro, Duque de Caxias and Nova Iguaçu; and between Niterói and Itaboraí. The distance among these pairs of cities is less than 50km and there are daily flows in high or low frequency. Figure 9 in Appendix 6.2 shows the human commuting for work or study in Rio de Janeiro, 2010.

Our results (Figs. 2, 3, 4, 5, and 6) showed that the reduced model is capable of properly reproducing the number of infected individuals for all pairs of cities. For Nova Iguaçu and Itaboraí, the fitting did not reach the peak of the outbreaks. A possible explanation for these two cities is that the peak value differs greatly from the incidence of the peak previous week, which may occur due to notifications being accumulated from one week to another. The fit also obtained reasonable values for the parameters (Table 2), including the ones simulating mobility.

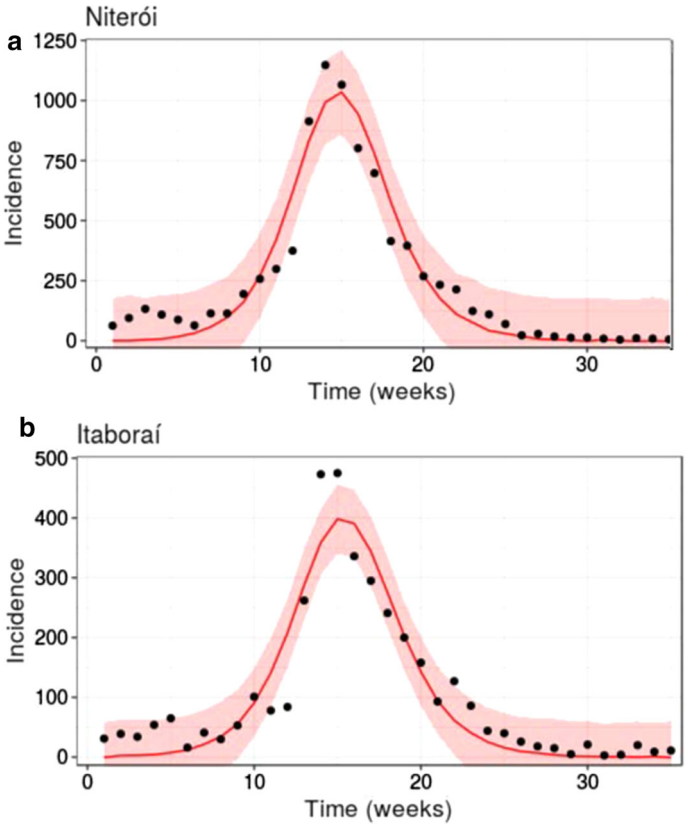


**Fig. 6** Result of fitting equations $I_1$ and $I_2$ from Model 9 to dengue incidence data from Niterói e Itaboraí, respectively, according to the parameters of Table 2. Black dots show the incidence per week, the solid lines (in red) show the results obtained from the model, and the region (filled with red) is the 95% confidence interval (CI) for the variation of the observations (color figure online)

The parameters $\beta_r$ and $\overline{\Omega_r}$ vary from 1.91 to 4.09 (weeks) and $\overline{\mu_{m_r}}$ has its value in the range [0.512 : 1.856] (weeks). The basic reproduction number $R_0 \approx 1.1$ is within the expected range, although it is slightly lower than what is generally found in the literature. A possible cause is the influence of mobility terms $d_{ij}$, which could increase the $R_0$ value by adding more cities in the spatial dynamics. Although, it is also important to mention the $R_0$ depends on which method is used to obtain its expression and how large is the data series being fitted. The more information is used in the fitting, the smaller is the estimated value of $R_0$ (see Sanches and Massad 2016).

For comparison purposes, Appendix 6.1 was included containing the results of fitting the data to Model 1 without human mobility, that is, considering that each population is isolated and there is no flow of people leaving or entering each city. In these simulations, in addition to vary the initial conditions, it was necessary to analyze different mosquito population sizes, as the real proportion of vectors compared to human population from each location is not known. We tested the proportion $N_m =$

$N_h$, $N_m = 2N_h$, $N_m = 3N_h$ and $N_m = 4N_h$, which required a greater computational effort.

Although the adjustments were similar, it is notable that the fitting of the $S_r I_r$ model got closer to the peak of the outbreaks. The $R_0$ was almost the same with both models, just slightly bigger in the one without the spatial dynamics. This was expected since in the $S_r I_r$ model, we only take into account the movement between two cities. A much larger mobility network would increase the $R_0$ value since it depends on the parameters $d_{rs}$. About the parameters $\beta_r$, $\overline{\Omega_r}$ and $\overline{\mu_{m_r}}$, the values obtained with the two models were totally different (see Table 2 and Table 3). We conclude that these parameters of Model 7 cannot be interpreted separately as in the model with bilinear incidence (Model 1). For the results in Table 2, the fitting was performed for two time series simultaneously in a modified model with nonlinear incidence rate, so it is necessary to consider the network and not the incidence of each city separately.

Regarding the mobility parameters, the estimated values were better than expected. We made the adjustment in order to analyze whether the model could capture the real movement between the locations. The values obtained for the pairs of cities: 1—Rio de Janeiro/Niterói, 2—Rio de Janeiro/Duque de Caxias and 3—Rio de Janeiro/Nova Iguaçu, precisely reflect the human movement between these cities as shown in Fig. 9. For 4—Duque de Caxias/Nova Iguaçu and 5—Niterói/Itaboraí, the simulations show a lower intensity of human movement, as it actually happens, but the values of the parameters were a little outside of the variation range. This may occur as a result of the lack of transport facilities that make the direct connection between cities in the metropolitan region (shown in Fig. 9), which could increase or decrease the direct flow among the pairs we analyzed.

Finally, we highlight that a realistic mobility network must involve several cities. Here, we deal with a prototype model with the objective of showing that the reduction in the order of the system can be used in an effective way to simulate indirectly transmitted infectious disease in a small mobility network without having to deal with vector population size and that the model with nonlinear incidence rate can be fitted to data. These results give us an indication that human mobility actually has influence on the spread of dengue and bring us perspectives for future studies combining more complex mobility networks and asymptotic techniques applied to analyze vector-borne diseases using real mobility data.

**Author Contributions** All authors contributed equally

**Funding** The second author (MP) is partially supported by CNPq 303253/2017-7 and FAPESP 2020/04813-0 (Brazil).

## Declarations

**Conflicts of interest** The authors declare that they have no conflict of interest.

**Availability of data and material** The data were obtained from Brazil's Information System for Notifiable Diseases (SINAN) da Saúde/SVS DATASUS (2020)

**Code availability** Adaptation of the code from **pomp** package described in King et al. (2015) and available in King (2022).

**Ethical Approval** Not applicable

**Consent to Participate** Not applicable

**Consent for Publication** Not applicable

## 6 Appendix

The numerical results below show that the trajectory of infected individuals from System (9), with the estimated parameters (Table 2), converges to an endemic state for all pairs of cities.

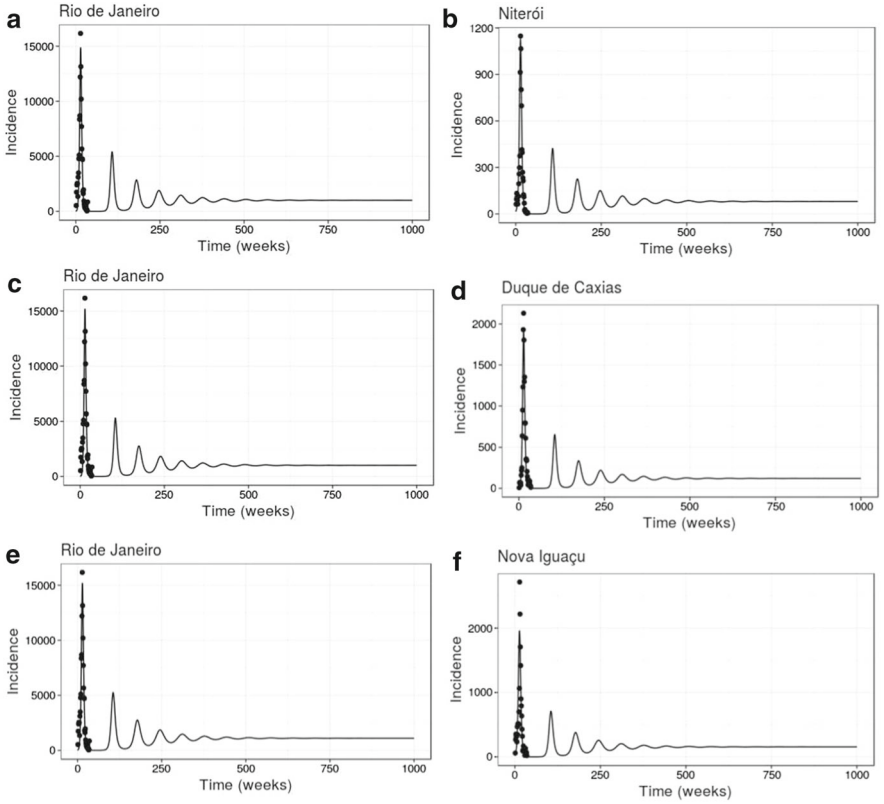


**Fig. 7** Convergence to endemic equilibrium. The plots show the curves of infected $I_1$ and $I_2$ for a period of 1000 weeks using the parameters presented in Table 2

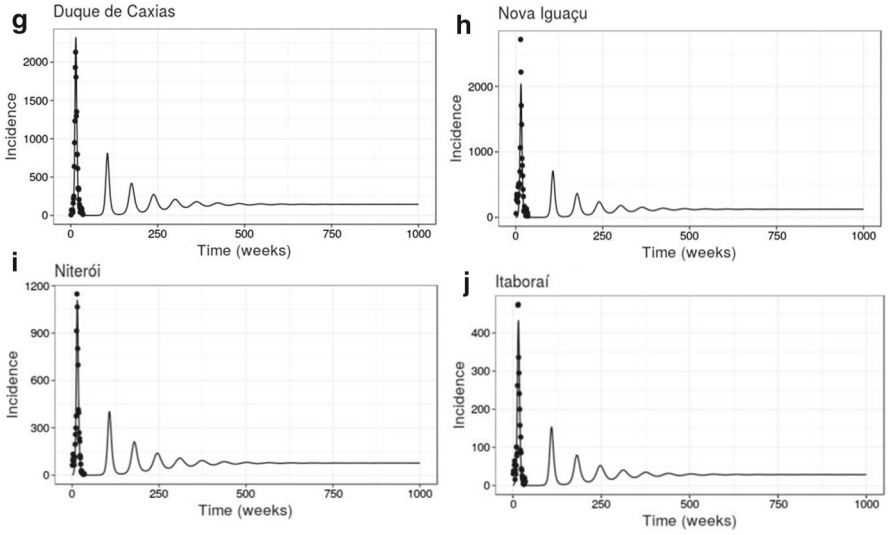


**Fig. 7** continued

### 6.1 Model Without Human Mobility

Considering the model SIRS$_m I_m$ (System 1, shown below), we run simulations assuming that each city is isolated, that is, without taking into account the flow of people among the cities.

$$\begin{aligned}
\mathrm{d}S/\mathrm{d}t &= \mu_h(N_h - S) - \beta S I_m/N_m \\
\mathrm{d}I/\mathrm{d}t &= \beta S I_m/N_m - (\gamma + \mu_h)I \\
\mathrm{d}R/\mathrm{d}t &= \gamma I - \mu_h R \\
\mathrm{d}S_m/\mathrm{d}t &= \mu_m(N_m - S_m) - \Omega S_m I/N_h \\
\mathrm{d}I_m/\mathrm{d}t &= \Omega S_m I/N_h - \mu_m I_m
\end{aligned}$$

The basic reproduction number $R_0$ for this model is obtained using the next generation matrix method van den Driessche (2017). The infected compartments are $I$ and $I_m$. At the disease free equilibrium, $(S, I, R, S_m, I_m) = (N_h, 0, 0, N_m, 0)$, the matrix $\mathbf{F}$ containing the appearance rates of new infections, and the matrix $\mathbf{V}$ with the other transitions among the compartments, are given, respectively, by:

$$\mathbf{F} = \begin{bmatrix} 0 & \frac{\beta N_h}{N_m} \\ \frac{\Omega N_m}{N_h} & 0 \end{bmatrix} \text{ and } \mathbf{V} = \begin{bmatrix} (\gamma + \mu_h) & 0 \\ 0 & \mu_m \end{bmatrix}. \tag{6}$$

Finally, the expression of $R_0$ is accomplished by calculating:

$$R_0 = \rho(\mathbf{F}\mathbf{V}^{-1}) = \sqrt{\frac{\beta\Omega}{\mu_m(\gamma + \mu_h)}}$$

**Table 3** Parameters obtained by fitting the infected equation $I$ from system 1 to dengue incidence data from Duque de Caxias, Itaboraí, Niterói, Nova Iguaçu and Rio de Janeiro

| Cities | Parameters (weeks) | | | | | | | | |
|---|---|---|---|---|---|---|---|---|---|
| | $\beta$ | $\Omega$ | $\mu_m$ | $\gamma$ | $S$ | $I$ | $S_m$ | $I_m$ | $R_0$ |
| Duque de Caxias | 8.882354 | 7.666129 | 7 | 7 | 682945 | 51.48 | 2566037 | 17.36 | 1.1788 |
| Itaboraí | 8.332454 | 7.567513 | 7 | 7 | 184748 | 9.70 | 219326 | 9.92 | 1.1344 |
| Niterói | 6.614968 | 11.59679 | 7 | 7 | 345768 | 21.34 | 976246 | 13.41 | 1.2512 |
| Nova Iguaçu | 9.593677 | 7.396838 | 7 | 7 | 616390 | 21.04 | 1595161 | 18.02 | 1.2034 |
| Rio de Janeiro | 8.461116 | 7.75405 | 7 | 7 | 5292017 | 175.12 | 12652420 | 174.98 | 1.1571 |

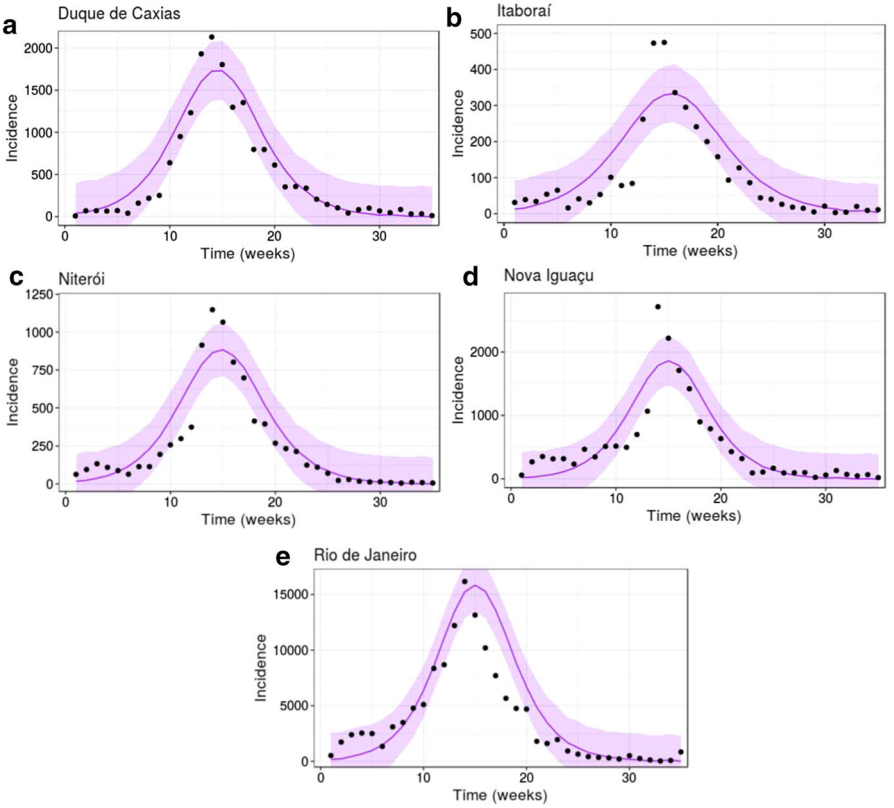


**Fig. 8** Fitting the solutions $I$ of the Model (1) to dengue incidence data for each city. Black dots show the incidence per week, the solid lines (in purple) show the results obtained from the model, and the region (filled with purple) is the 95% confidence interval (CI) for the variation of the observations (color figure online)

Table (3) contains the values of the estimated parameters, and Fig. (8) shows the fitting.

### 6.2 Commuting Among Rio de Janeiro Cities

see Fig. 9

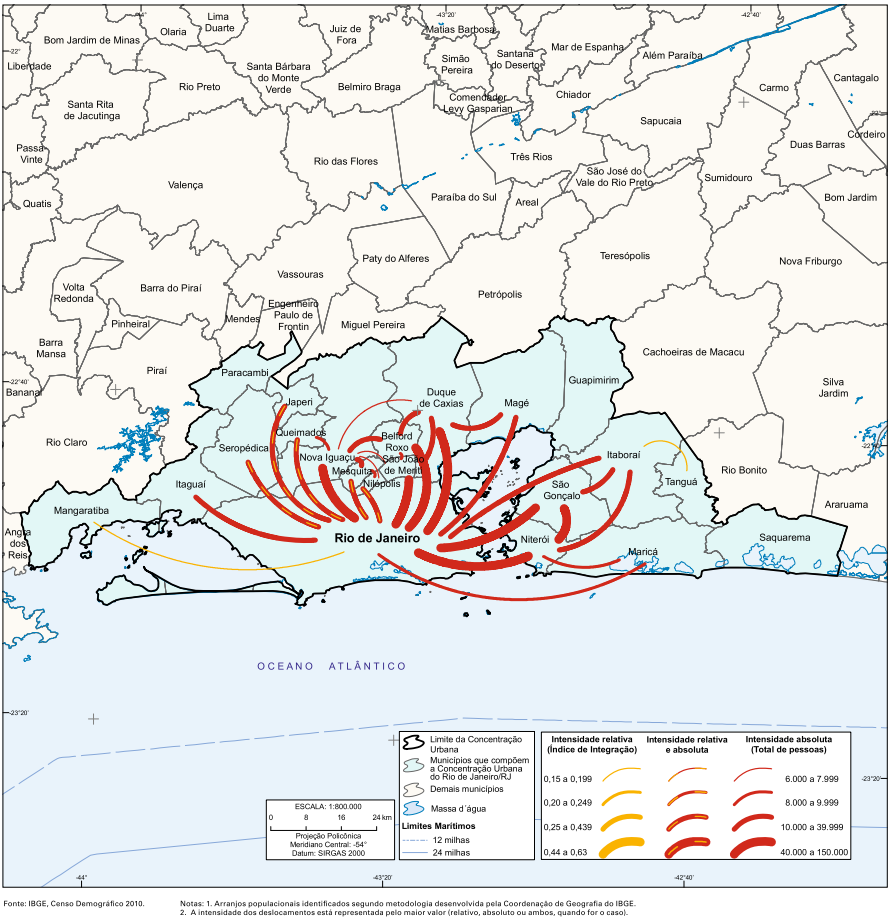


**Fig. 9** Intensity of commuting for work and study in the Urban Concentration of Rio de Janeiro/RJ. The connections in red show the absolute intensity (total of people). IBGE, 2010 Brazilian Census BRASIL (2015) (color figure online)

## References

Amaku M, Azevedo F, Burattini MN, Coelho GE, Coutinho FAB, Greenhalgh D, Lopez L, Motitsuki R, Wilder-Smith A, Massad E (2016) Magnitude and frequency variations of vector-borne infection outbreaks using the Ross-Macdonald model: explaining and predicting outbreaks of dengue fever. Epidemiol Infect 144(16):3435–3450

Barmak DH, Dorso CO, Otero M, Solari HG (2011) Dengue epidemics and human mobility. Phys Rev E 84(1):011901
Bhatt S, Gething PW, Brady OJ, Messina JP, Farlow AW, Moyes CL, Drake JM, Brownstein JS, Hoen AG, Sankoh O et al (2013) The global distribution and burden of dengue. Nature 496(7446):504–507
Boccia T, Burattini M, Coutinho F, Massad E (2014) Will people change their vector-control practices in the presence of an imperfect dengue vaccine? Epidemiol Infect 142(3):625–633
Bomfim R, Pei S, Shaman J, Yamana T, Makse HA, Andrade JS Jr, Lima Neto AS, Furtado V (2020) Predicting dengue outbreaks at neighbourhood level using human mobility in urban areas. J R Soc Interface 17(171):20200691
BRASIL I (2015) Arranjos populacionais e concentrações urbanas do brasil. https://biblioteca.ibge.gov.br/visualizacao/livros/liv93202.pdf, accessed on June 2022
Brauer F, Castillo-Chavez C, Mubayi A, Towers S (2016) Some models for epidemics of vector-transmitted diseases. Infect Dis Model 1(1):79–87
Brockmann D, Helbing D (2013) The hidden geometry of complex, network-driven contagion phenomena. Science 342(6164):1337–1342
Brockmann D, David V, Gallardo AM (2009) Human mobility and spatial disease dynamics. Reviews of nonlinear dynamics and complexity, vol 2, pp 1–24
Burattini MN, Lopez LF, Coutinho FA, Siqueira-Jr JB, Homsani S, Sarti E, Massad E (2016) Age and regional differences in clinical presentation and risk of hospitalization for dengue in Brazil, 2000–2014. Clinics 71(8):455–463
da Saúde/SVS DATASUS M (2020) Sistema de Informação de Agravos de Notificação - Sinan Net. http://tabnet.datasus.gov.br/cgi/deftohtm.exe?sinannet/cnv/denguerj.def, accessed on July 2020
dos Santos BC, Sartori LM, Peixoto C, Bevilacqua JS, Oliva SM (2018) Prospective study about the influence of human mobility in dengue transmission in the state of Rio de Janeiro. Modeling. Dynamics, Optimization and Bioeconomics III, Springer, pp 419–427
Ducrot A, Magal P, Seydi O (2017) Singular perturbation for an abstract non-densely defined Cauchy problem. J Evolution Equ 17(3):1089–1128
Gubler DJ (2002) Epidemic dengue/dengue hemorrhagic fever as a public health, social and economic problem in the 21st century. Trends Microbiol 10(2):100–103
Hartmann C (2008) Singularly perturbed differential equations
Hethcote HW, Van den Driessche P (1991) Some epidemiological models with nonlinear incidence. J Math Biol 29(3):271–287
Iggidr A, Koiller J, Penna MLF, Sallet G, Silva MA, Souza M (2017) Vector borne diseases on an urban environment: the effects of heterogeneity and human circulation. Ecol Complex 30:76–90
King AA (2022) Introduction to inference: parameter estimation. Fitting deterministic dynamical epidemiological models to data. https://kingaa.github.io/short-course/parest/parest.html, Accessed on June 2022
King AA, Nguyen D, Ionides EL (2015) Statistical inference for partially observed Markov processes via the R package pomp. https://kingaa.github.io/pomp/
King JG, Souto-Maior C, Sartori LM, Maciel-de Freitas R, Gomes MGM (2018) Variation in Wolbachia effects on Aedes mosquitoes as a determinant of invasiveness and vectorial capacity. Nat Commun 9(1):1–8
Kiss IZ, Green DM, Kao RR (2006) Infectious disease control using contact tracing in random and scale-free networks. J R Soc Interface 3(6):55–62
Kraemer MU, Sinka ME, Duda KA, Mylne AQ, Shearer FM, Barker CM, Moore CG, Carvalho RG, Coelho GE, Van Bortel W et al (2015) The global distribution of the arbovirus vectors *Aedes aegypti* and Ae albopictus. elife 4:e08347
Liang G, Gao X, Gould EA (2015) Factors responsible for the emergence of arboviruses; strategies, challenges and limitations for their control. Emerg Microbes Infect 4(1):1–5
Liu-Helmersson J, Quam M, Wilder-Smith A, Stenlund H, Ebi K, Massad E, Rocklöv J (2016) Climate change and Aedes vectors: 21st century projections for dengue transmission in Europe. EBioMedicine 7:267–277
Massad E, Ma S, Chen M, Struchiner CJ, Stollenwerk N, Aguiar M (2008) Scale-free network of a dengue epidemic. Appl Math Comput 195(2):376–381
Newman ME (2003) The structure and function of complex networks. SIAM Rev 45(2):167–256

Peixoto PS, Marcondes D, Peixoto C, Oliva SM (2020) Modeling future spread of infections via mobile geolocation data and population dynamics. An application to COVID-19 in Brazil. PloS ONE 15(7):e0235732

Pereira M, Oliva S, Sartori L (2020) Time-scale analysis nonlocal diffusion systems, applied to disease models. Math Methods Appl Sci 3(15):8632–8643. https://doi.org/10.1002/mma.6522

Precioso AR, Palacios R, Thomé B, Mondini G, Braga P, Kalil J (2015) Clinical evaluation strategies for a live attenuated tetravalent dengue vaccine. Vaccine 33(50):7121–7125

Rocha F, Aguiar M, Souza M, Stollenwerk N (2013) Time-scale separation and centre manifold analysis describing vector-borne disease dynamics. Int J Comput Math 90(10):2105–2125

Rodriguez-Barraquer I, Cordeiro MT, Braga C, de Souza WV, Marques ET, Cummings DA (2011) From re-emergence to hyperendemicity: the natural history of the dengue epidemic in Brazil. PLoS Negl Trop Dis 5(1):e935

Saba H, Vale VC, Moret MA, Miranda JGV (2014) Spatio-temporal correlation networks of dengue in the state of Bahia. BMC Public Health 14(1):1085

Sanches RP, Massad E (2016) A comparative analysis of three different methods for the estimation of the basic reproduction number of dengue. Infect Dis Model 1(1):88–100

Souza MO (2014) Multiscale analysis for a vector-borne epidemic model. J Math Biol 68(5):1269–1293

van den Driessche P (2017) Reproduction numbers of infectious disease models. Infect Dis Model 2(3):288–303

Wang L, Zhao H, Oliva SM, Zhu H (2017) Modeling the transmission and control of Zika in Brazil. Sci Rep 7(1):1–14